International Journal of Research Publication and Reviews

Journal homepage: www.ijrpr.com ISSN 2582-7421

Determine the Depositional Environment of Limestones Using Major Oxide Data – A Review

Osama Rahil Shaltami

Department of Earth Sciences, Faculty of Science, University of Benghazi, Libya

ABSTRACT

For every field of geology, assessing the depositional environment is crucial. The sediments' fossil, sedimentary, geochemical, or geophysical characteristics can all be used to determine the depositional environment. This paper reviewed how to use the major oxides to identify the depositional environment of limestones. There are several parameters previously used for this purpose, such as $Al_2O_3/(Al_2O_3+Fe_2O_3)$, Ca/(Ca+Fe), Na_2O/K_2O, Ca/Mg, Mg/Ca, Fe_2O_3/TiO_2, Fe/(Ca+Mg), Ti/Al, Al/(Al+Fe), Mn*, Fe_{HR}/Fe_T and Fe/Al. New parameters (S/Ca ratio) and plots (P versus Fe and P versus Ca) are proposed in this paper.

Keywords: Major Oxides, Depositional Environment, Redox Condition, Limestone.

1. Introduction

Sedimentary cycle is a set of processes (weathering, erosion, transportation, sedimentation, and diagenesis) that lead to the formation of sedimentary rocks (Boggs Jr, 2005). Sedimentary rocks' characteristics are the result of biological, chemical, and physical processes. Sediments are placed on a portion of the earth's surface known as the depositional environment, which has specific chemical, biological, and physical properties. Continental (terrestrial), transitional (marginal marine) and marine environments are the three different classes of depositional environments (e.g., Tucker, 2001; Boggs Jr, 2005; Leeder, 2011; Long, 2017; Nichols, 2023). Fluvial, desert, lacustrine, and glacial environments are the four main categories of continental environments. There are six major types of transitional environments, they are lagoonal, estuarine, deltaic, tidal flat, beach, and barrier island. Marine environments are classified as shallow marine, deep marine and reef (Tucker, 2001).

In the three distinct depositional environments (continental, transitional and marine environments) limestones can form. There is a strong genetic correlation between sedimentary rocks' characteristics and depositional setting. In geological branches such as sedimentology, stratigraphy, paleontology, geochemistry, and geophysics, the determination of depositional environments is crucial (e.g., Hadler et al., 2013; Lamourou et al., 2017; Bataller et al., 2021; Shaltami, 2024).

Numerous parameters, including fossil content (e.g., Irmis et al., 2013; Özer and Kahrıman, 2019; Wang et al., 2023), sedimentological characteristics (e.g., Ojo and Akande, 2009; Momta et al., 2015), chemical composition (e.g., Ratcliffe et al., 2007; Zhang et al., 2013; Khan et al., 2023), and geophysical data (e.g., Pigott et al., 2013; Teama et al., 2018; Khoshnoodkia et al., 2022), can be used to define the depositional environment. Geochemists use several parameters to determine the depositional environment, such as major oxides, trace elements (e.g., Ratcliffe et al., 2007; Dhannoun and Al-Dlemi, 2013; He et al., 2019; Shaltami, 2024), and biomarkers (e.g., Peters et al., 2005; Zhou and Huang, 2008; Fang et al., 2016; Shaltami, 2022). This paper reviewed major oxide data-based methods for assessing the depositional environment of limestones. The author suggested new parameters and plots to assess water depth and redox conditions.

Major elements, which include Si, Al, Ca, Mg, Na, K, Ti, Fe, Mn, S, and P, are the main component of the earth's crust, as their concentration reaches more than 95%. X-ray fluorescence (XRF) and inductively coupled plasma (ICP) are typically used in the major element geochemistry. Major elements are most frequently measured as oxides, specifically as SiO_2, TiO_2, Al_2O_3, Fe_2O_3, MnO, MgO, CaO, Na_2O, K_2O, P_2O_5, and SO_3.

2. Depositional Environment

2.1. Classes

Multiple parameters, including $Al_2O_3/(Al_2O_3+Fe_2O_3)$ (He *et al.*, 2019), Ca/(Ca+Fe) (Zhang *et al.*, 2013; Khan et al., 2023), Na_2O/K_2O (Gao et al., 2022), Ca/Mg and Mg/Ca ratios (Ehinola et al., 2016), can be utilized to determine the depositional environment of limestones. The $Al_2O_3/(Al_2O_3+Fe_2O_3)$ ratios in the continental margin and in the oceanic basin range from 0.5 to 0.9 and 0.4 to 0.7, respectively (He *et al.*, 2019). Fresh water, brackish water and saline water show different Ca/(Ca+Fe) ratios (<0.4, 0.4 to 0.8, and 0.8, respectively, Khan et al., 2023). Limestone formation stability in the depositional environment is influenced by the Ca/Mg ratio. In the salinized settings, the Mg/Ca ratio naturally increases as seawater evaporates (Ehinola et al., 2016). Mg in marine limestones can redistribute as a result of alteration, especially when fresh meteoric water percolates through the rock.Ca is insensitive to these alterations (Averyt et al., 2003; Bayon et al., 2007). In the depositional environment, K and Na found in water are adsorbed by clay minerals (Gerdes et al., 2002). Both K and Na are adsorbed more readily in higher salinity water, but Na is adsorbed more hardly than K. Consequently, one useful indicator of the salinity of the limestone depositional environment is the Na_2O/K_2O ratio. This ratio decreases as water becomes more salinized (Gao et al., 2022).

There are several discrimination diagrams used to conclude the depositional environment of limestone such as the binary plots of MgO versus FeO (Fig. 1, Ratcliffe et al., 2007), log MgO/Al_2O_3 versus log K_2O/Al_2O_3 (Fig. 2, El-Desoky et al., 2015), Fe+Ca versus Ca (Fig. 3, He et al., 2019), Fe_2O_3 versus Al_2O_3 (Fig. 4, Zhang et al., 2017), and $Al_2O_3/(Al_2O_3+Fe_2O_3)$ versus Fe_2O_3/TiO_2 (Fig. 5, He et al., 2019) and the ternary plot of $MgO-Fe_2O_3-SiO_2/Al_2O_3$ (Fig. 6, Ratcliffe et al., 2007).

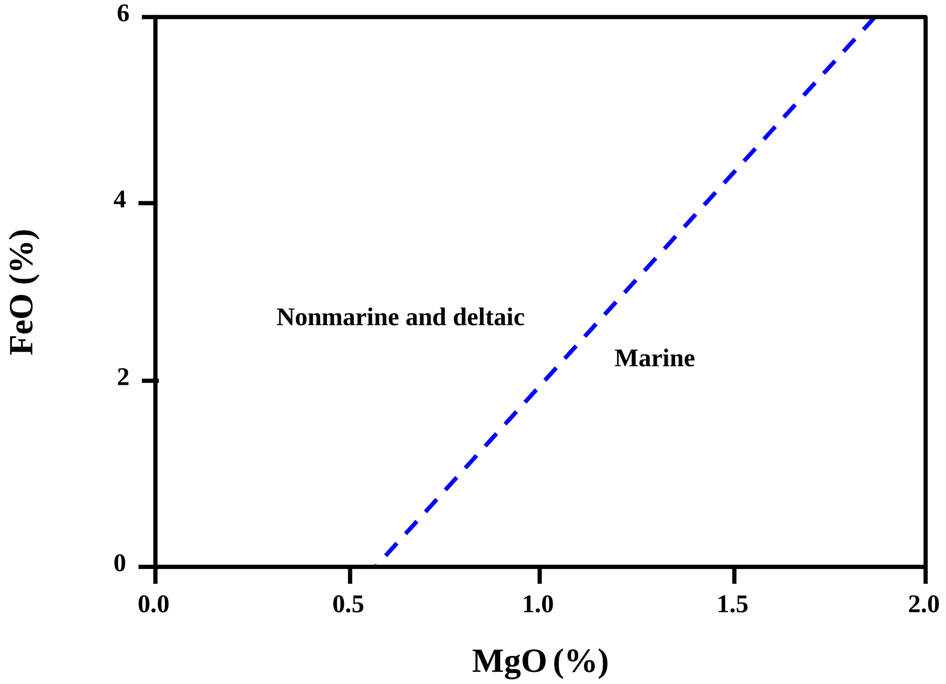

Fig. 1: Binary plot of MgO vs. FeO (after Ratcliffe et al., 2007).

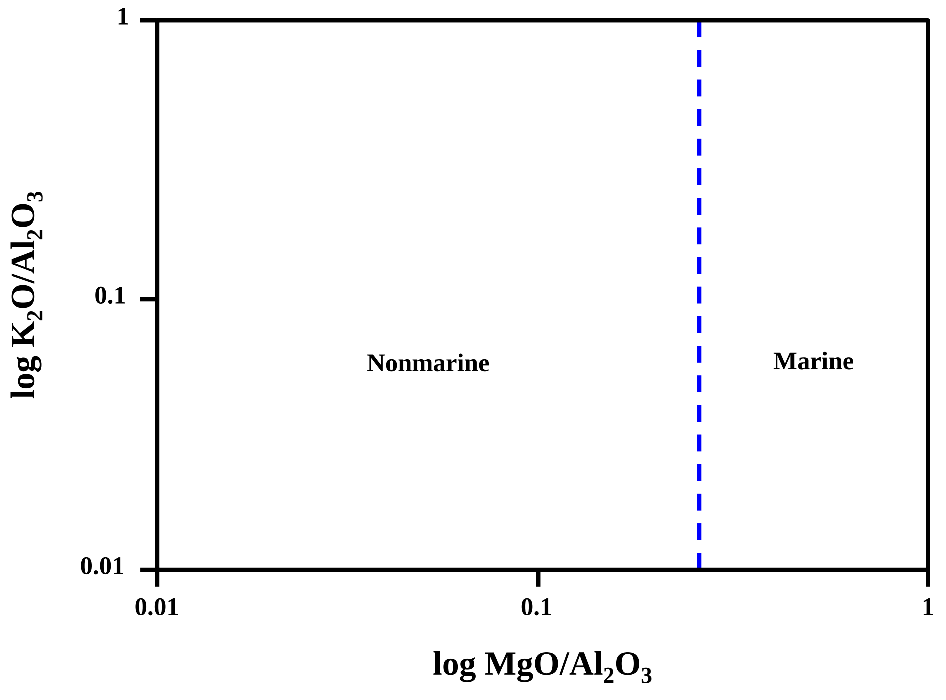

Fig. 2: Binary plot of log MgO/Al_2O_3 vs. log K_2O/Al_2O_3 (after El-Desoky et al., 2015).

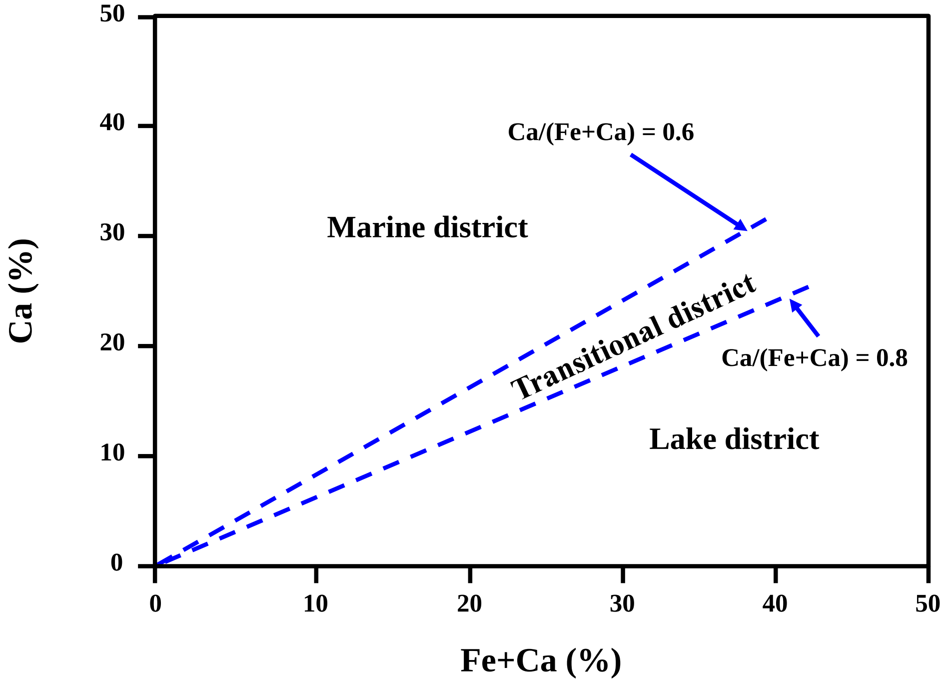

Fig. 3: Binary plot of Fe+Ca vs. Ca (after He et al., 2019).

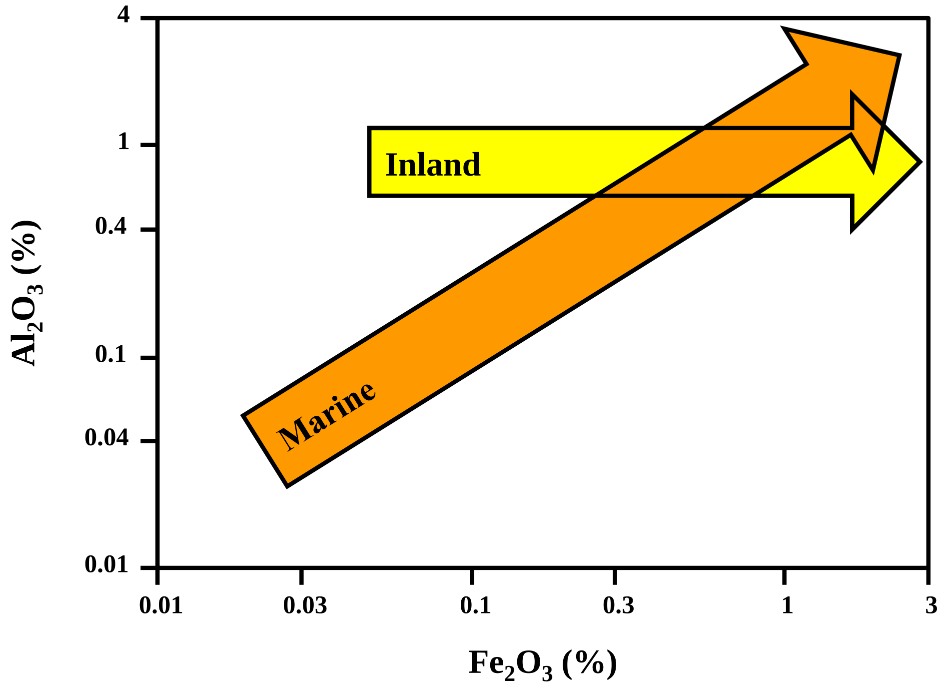

Fig. 4: Binary plot of Fe_2O_3 vs. Al_2O_3 (after Zhang et al., 2017).

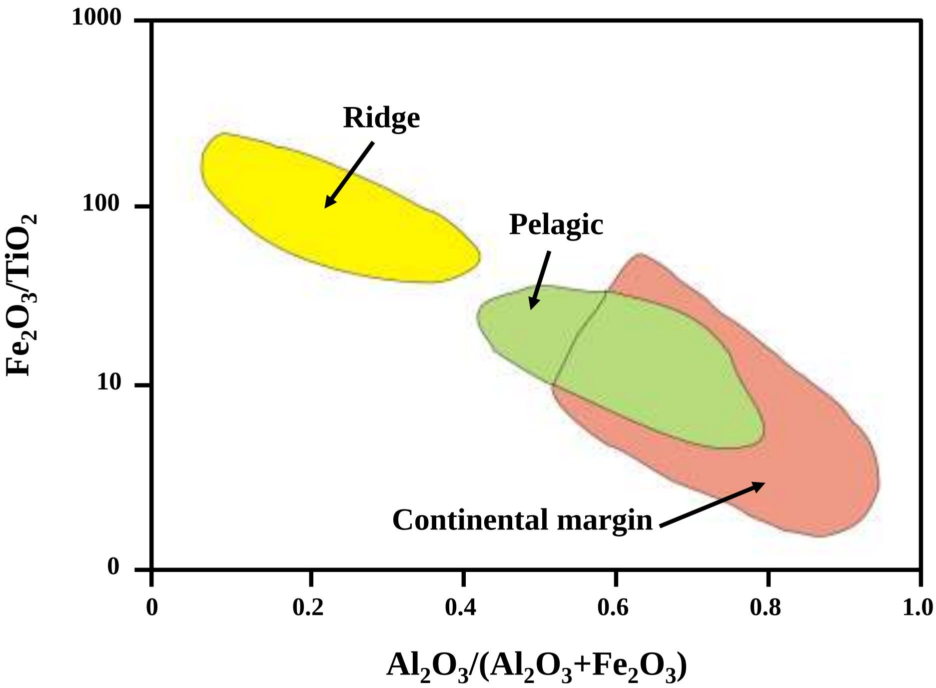

Fig. 5: Binary plot of $Al_2O_3/(Al_2O_3+Fe_2O_3)$ vs. Fe_2O_3/TiO_2 (after He et al., 2019).

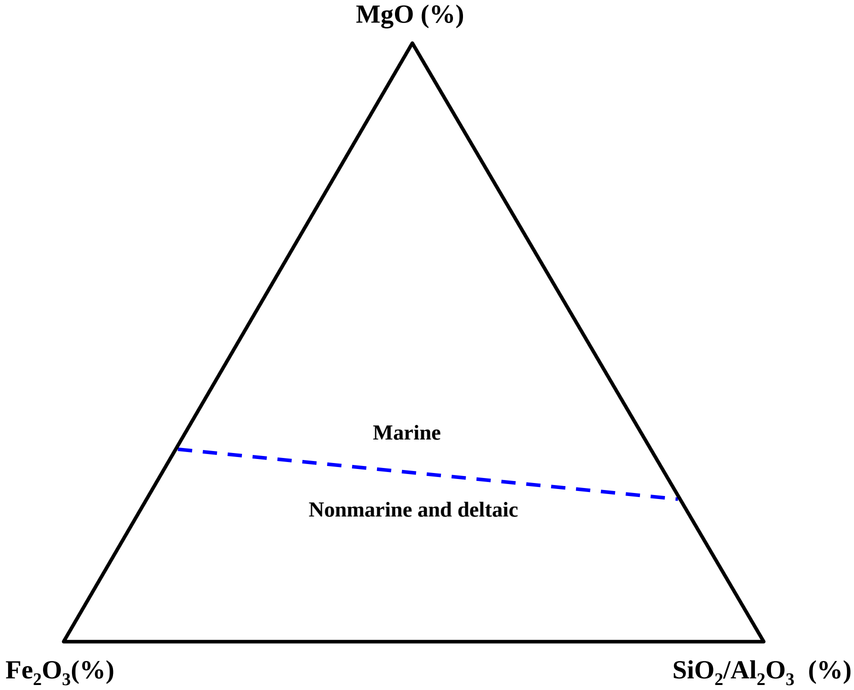

Fig. 6: Ternary plot of MgO-Fe_2O_3-SiO_2/Al_2O_3 (after Ratcliffe et al., 2007).

2.3. Water Depth

According to Khan *et al.,* (2023) the Fe/(Ca+Mg) ratio can be used to determine the water depth. The high ratios indicate deep water conditions. The water depth is ascertained using a number of binary plots, including Al_2O_3 versus P_2O_5 (Fig. 7, Dhannoun and Al-Dlemi, 2013), Ca versus Fe (Fig. 8, Naseem et al., 2005) and CaO versus MgO (Fig. 9, Naseem et al., 2005). Moreover, two discrimination diagrams are proposed in this work to characterize the water depth. These diagrams are the binary plots of P versus Fe (Fig. 10) and P versus Ca (Fig. 11).

2.3. Terrigenous Input

The limestone depositional settings were significantly influenced by the availability of terrigenous material. Some elements (Fe and Al) that were readily liberated by weathering precipitated when there was a change in the pH of seawater, while the limestone became enriched in elements (Si) that were less affected by weathering (Gao et al., 2022). The most trustworthy geochemical proxy for determining the intensity of terrestrial source is the Ti/Al ratio (Murphy et al., 2000). Low ratios suggest low terrestrial input. Moreover, the terrestrial origin can be inferred when the Al/(Al+Fe) ratio is more than 4 (Liu et al., 2015).

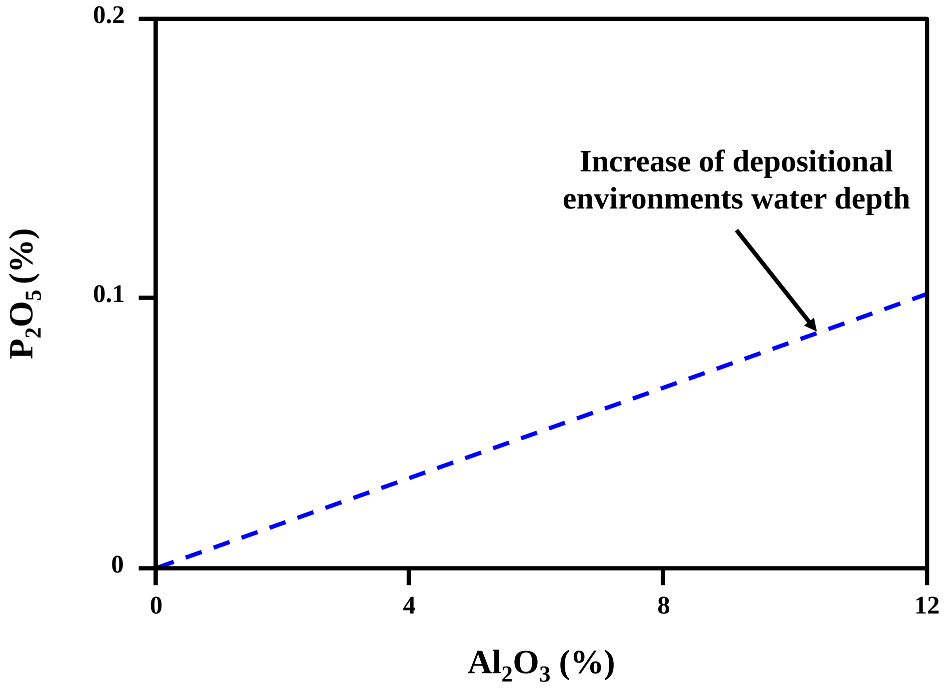

Fig. 7: Binary plot of Al_2O_3 vs. P_2O_5 (after Dhannoun and Al-Dlemi, 2013).

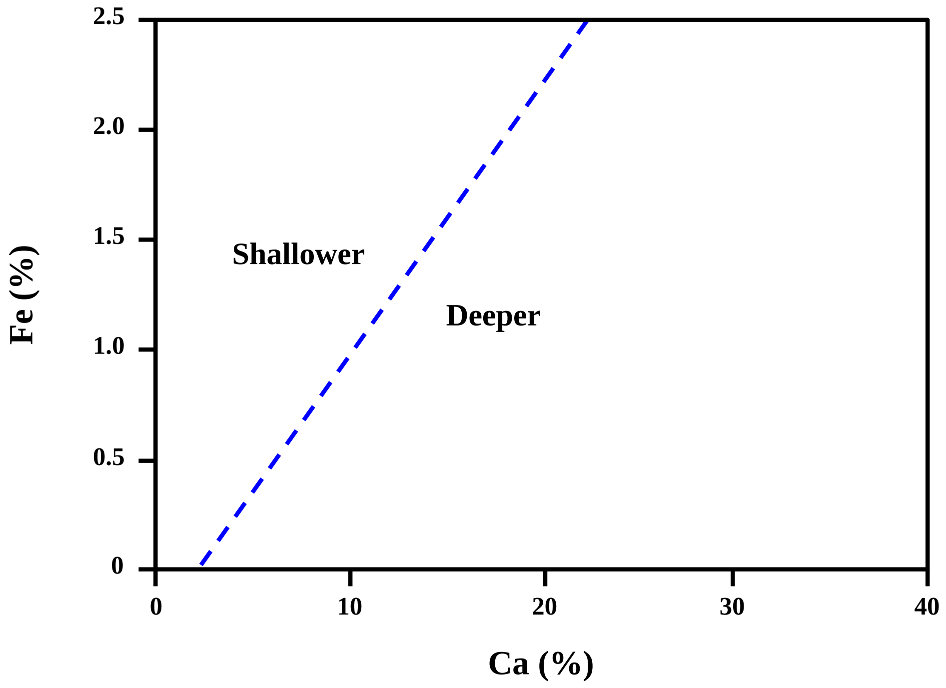

Fig. 8: Binary plot of Ca vs. Fe (after Naseem et al., 2005).

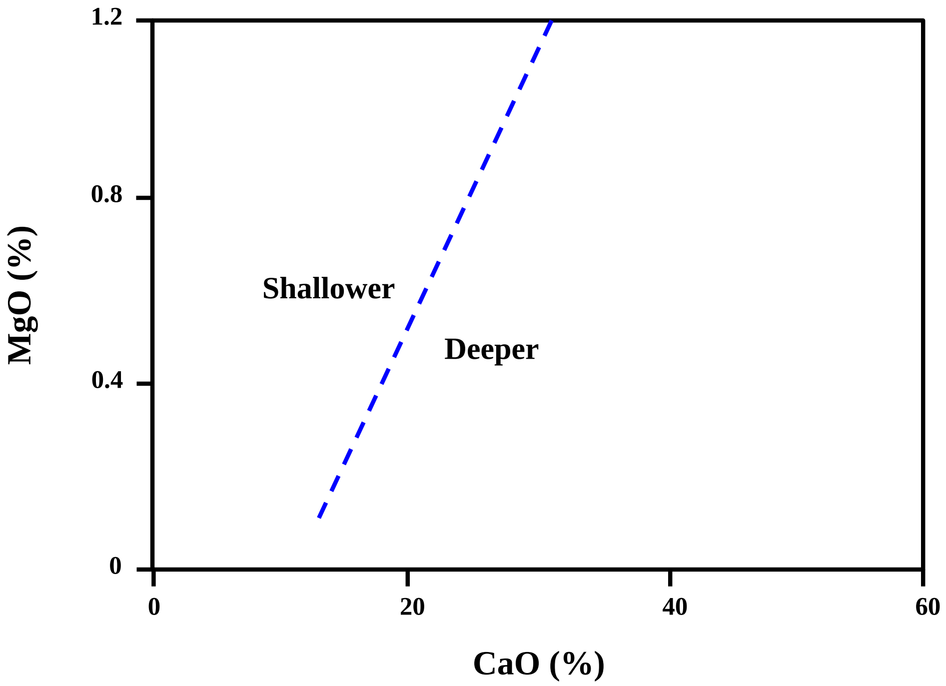

Fig. 9: Binary plot of CaO vs. MgO (after Naseem et al., 2005).

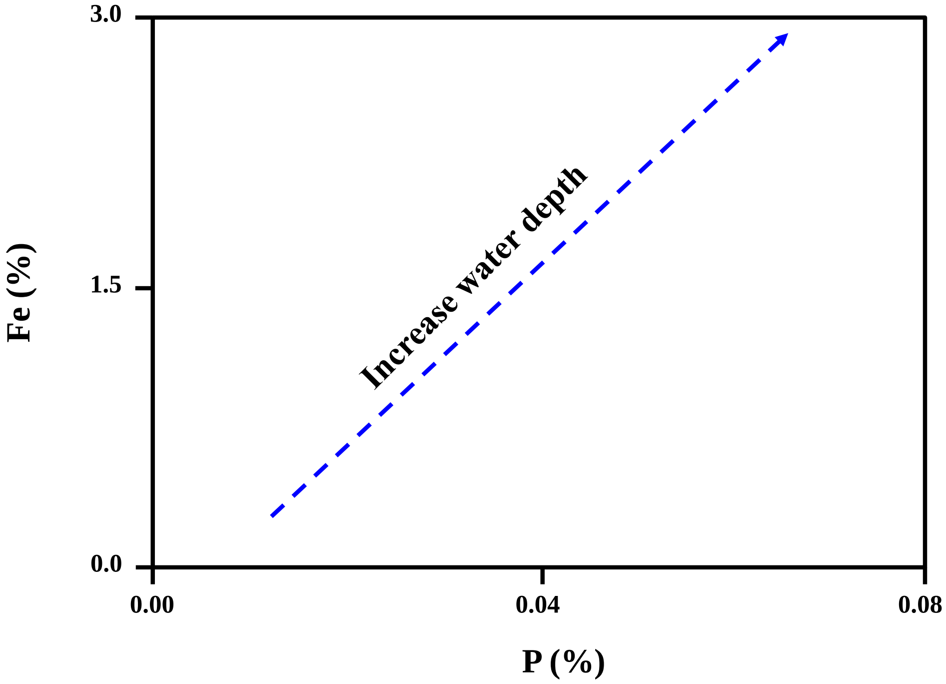

Fig. 10: Binary plot of P vs. Fe (proposed by the author).

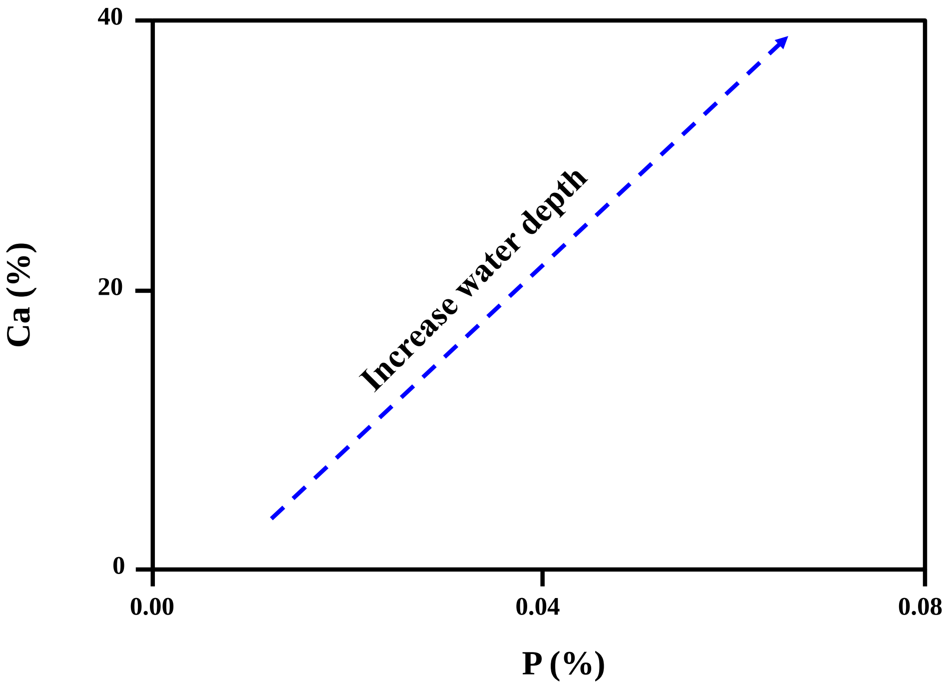

Fig. 11: Binary plot of P vs. Ca (proposed by the author).

2.4. Redox Condition

Identifying redox conditions is a primary objective in many investigations of the depositional environment. For limestones, a variety of redox parameters are available, such as Mn* (Machhour et al., 1994; Bellanca et al., 1996), highly reactive iron/total iron (Fe_{HR}/Fe_T, Poulton and Canfield, 2011) and Fe/Al (Lyons and Severmann, 2006). Mn* is calculated using the following equation: $Mn^* = \log((Mn_{sample}/Mn_{shale})/(Fe_{sample}/Fe_{shale})$. Wedepohl (1978) determined the values of Mn_{shale} (600 ppm) and Fe_{shale} (46150 ppm) used in this equation. Positive Mn* values indicate oxic conditions, while anoxic conditions display negative values (Machhour et al., 1994; Bellanca et al., 1996). When reconstructing the diagenetic evolution, Mn and Fe can be valuable indicators. Marine environments can lead to Mn and Fe enrichment (Gao et al., 2022). The low Fe_2O_3 values suggest deposition in anoxic conditions that that Fe^{2+} is not precipitated to Fe^{3+} and is therefore leached away (Brand, 1983). The low SO_3 values is most likely caused by the reducing conditions that pervaded these peaceful, low-energy settings and the quick rate of sulfate reduction (Ehinola et al., 2016). The typical Fe_{HR}/Fe_T ratios for oxic condition, suboxic condition, and anoxic condition are <0.22, 0.22-0.38, and >0.38, respectively (Poulton and Canfield, 2011). Fe/Al ratios of >0.5-0.6 are thought to be suggestive of euxinic conditions (Lyons and Severmann, 2006). A new parameter (S/Ca ratio) was suggested by the author to ascertain the redox conditions. Low values denote anoxic conditions, whereas high values imply oxic conditions.

3. Conclusions

There are four key points that sum up this paper's conclusions:

1) A number of parameters ($Al_2O_3/(Al_2O_3+Fe_2O_3)$, Ca/(Ca+Fe), Na_2O/K_2O, Ca/Mg and Mg/Ca ratios) and diagrams (MgO versus FeO, log MgO/Al_2O_3 versus log K_2O/Al_2O_3, Fe+Ca versus Ca, Fe_2O_3 versus Al_2O_3, and $Al_2O_3/(Al_2O_3+Fe_2O_3)$ versus Fe_2O_3/TiO_2 and of MgO-Fe_2O_3-SiO_2/Al_2O_3) are used to identify the depositional environment class.

2) Water depth is determined using the Fe/(Ca+Mg) ratio and the binary plots of Al_2O_3 versus P_2O_5, Ca versus Fe, CaO versus MgO, P versus Fe and P versus Ca.

3) The Ti/Al and Al/(Al+Fe) ratios are considered the most important indicator of terrestrial input.

4) The redox conditions can be assessed using a number of parameters, including Mn*, Fe_{HR}/Fe_T, Fe/Al and S/Ca ratios.

References

Averyt, K.B., Paytan, A. and Li, G. (2003): A precise, high-throughput method for determining Sr/Ca, Sr/Ba, and Ca/Ba ratios in marine barite. Geochemistry, Geophysics, Geosystems; 4(4): 1039.

Bataller, F.J., McDougall, N.D., Moscariello, A., Gil-Ortiz, M. and de Paula, B.C. (2021): Late Ordovician deglaciation of the Murzuq Basin (SW Libya): a core to seismic-scale characterization of the depositional environments and sedimentary architecture. Marine and Petroleum Geology; 134: 105335.

Bayon, G., Pierre, C., Etoubleau, J., Voisset, M., Cauquil, E., Marsset, T., Sultan, N., Le Drezen, E. and Fouquet, Y. (2007): Sr/Ca and Mg/Ca ratios in Niger Delta sediments: Implications for authigenic carbonate genesis in cold seep environments. Marine Geology; 241(1-4): 93-109.

Bellanca, A., Claps, M., Erba, E., Masetti, D., Neri, R., Premoli-Silva, I. and Venezia, F. (1996): Orbitally induced limestone/marlstone rhythms in the Albian-Cenomanian Cismon section (Venetian región, northern Italy): sedimentology, calcareous and siliceous plankton distribution, elemental and isotope geochemistry. Palaeogeography, Palaeoclimatology, Palaeoecology; 126: 227-260.

Boggs Jr, S. (2005): Principles of sedimentology and stratigraphy. 4^{th} edition, Pearson; 688p.

Brand, U. (1983): Mineralogy and geochemistry of Deep Sea clay in the Atlantic Ocean and adjacent seas and ocean. Geological Society of America Bulletin; 76: 803-832.

Dhannoun, H.Y. and Al-Dlemi, A.M.S. (2013): The relation between Li, V, P_2O_5, and Al_2O_3 contents in marls and mudstones as indicators of environment of deposition. Arabian Journal of Geosciences; 6: 817-823.

Ehinola, O.A., Ejeh, O.I. and Oderinde, O.J. (2016): Geochemical characterization of the Paleocene Ewekoro Limestone Formation, SW Nigeria: Implications for provenance, diagenesis and depositional environment. Geomaterials; 6: 61-77.

El-Desoky, H., El-Rahmany, M., Farouk, S., Ahmed Khalil, A. and Fahmy, W. (2015): Geochemical characteristics of goethite-bearing deposits in the Dakhla – Kharga Oases, Western Desert, Egypt. International Journal of Scientific Engineering and Applied Science (IJSEAS); 1(8): 72-85.

Fang, R.H., Wang, T.G., Li, M.J., Xiao, Z.Y., Zhang, B.S., Huang, S.Y., Shi, S.B., Wang, D.W. and Deng, W.L. (2016): Dibenzothiophenes and benzo[b] naphthothiophenes: Molecular markers for tracing oil filling pathways in the carbonate reservoir of the Tarim Basin, NW China. Organic Geochemistry; 91: 68-80.

Gao, J., Lv, D.W., van Loon, A.J. and Wu, D. (2022): Geochemical, mineralogical, and petrological analyses for the interpretation of the sedimentary environment of the Middle-Late Ordovician Majiagou Formation (northern China) as a tool for more effective gas exploration. Petroleum Science; 19(6): 2519-2532.

Gerdes, A., Montero, P., Bea, F., Fershater, G., Borodina, N., Osipova, T. and Shardakova, G. (2002): Peraluminous granites frequently with mantle-like isotope compositions: the continental-type Murzinka and Dzhabyk batholiths of the eastern Urals. International Journal of Earth Sciences; 91(1): 3-19.

Hadler, P., Dias, A.S. and Bauermann, S.G. (2013): Multidisciplinary studies of Southern Brazil Holocene: Archaeological, palynological and paleontological data. Quaternary International; 305: 119-126.

He, C., Ji, L., Su, A., Wu, Y., Zhang, M., Zhou, S., Li, J., Hao, L. and Ma, Y. (2019): Source-rock evaluation and depositional environment of black shales in the Triassic Yanchang Formation, southern Ordos Basin, north-central China. Journal of Petroleum Science and Engineering; 173: 899-911.

Irmis, R.B., Whiteside, J.H. and Kammerer, C.F. (2013): Non-biotic controls of observed diversity in the paleontologic record: An example from the Permo-Triassic Karoo Basin of South Africa. Palaeogeography, Palaeoclimatology, Palaeoecology; 372: 62-77.

Khan, D., Zijun, L., Qiu, L., Kuiyuan, L., Yongqiang, Y., Cong, N., Bin, L., Li, X. and Habulashenmu, Y. (2023): Mineralogical and geochemical characterization of lacustrine calcareous shale in Dongying Depression, Bohai Bay Basin: Implications for paleosalinity, paleoclimate, and paleoredox conditions. Geochemistry, In Press.

Khoshnoodkia, M., Rahmani, O., Adabi, M.H., Hosseini-Barzi, M. and Mahdi, T.A. (2022): Depositional environment, seismic stratigraphy, and Sr-isotope geochronology, Bangestan reservoir, Ahwaz oilfield, SW Iran. Journal of Petroleum Science and Engineering; 208(C): 109629.

Lamourou, A., Touir, J. and Fagel, N. (2017): Reconstructing the Holocene depositional environments along the northern coast of Sfax (Tunisia): Mineralogical and sedimentological approaches. Journal of African Earth Sciences; 129: 713-727.

Leeder, M. (2011): Sedimentology and sedimentary basins: From turbulence to tectonics. 2^{nd} edition, Wiley-Blackwell; 794p.

Liu, Z.H., Zhuang, X.G., Teng, G.E., Xie, X.M., Yin, L.M., Bian, L.Z., Feng, Q. and Algeo, T. (2015): The Lower Cambrian Niutitang Formation at Yangtiao (Guizhou, SW China): Organic matter enrichment, source rock potential, and hydrothermal influences. Journal of Petroleum Geology; 38: 411-432.

Long, C. (2017): Principles of sedimentology. Larsen and Keller Education; 292p.

Lyons, T.W. and Severmann, S. (2006): A critical look at iron paleoredox proxies: New insights from modern euxinic marine basins. Geochimica et Cosmochimica Acta; 70(23): 5698-5722.

Machhour, L., Philip, J. and Oudin, J.L. (1994): Formation of laminate deposits in anaerobic-dysaerobic marine environments. Marine Geology; 117: 287-302.

Momta, P.S., Omoboh J.O. and Odigi, M.I. (2015): Sedimentology and depositional environment of D2 sand in part of Greater Ughelli Depobelt, onshore Niger Delta, Nigeria. American Journal of Engineering and Applied Sciences; 8(4): 556-566.

Murphy, A.E., Sageman, B.B., Hollander, D.J., Lyons, T.W. and Brett, C.E. (2000): Black shale deposition and faunal overturn in the devonian appalachian basin: clastic starvation, seasonal water-column mixing, and efficient biolimiting nutrient recycling. Paleoceanography; 15(3): 280-291.

Naseem, S., Naseem, S. and Sheikh, S.A. (2005): Geochemical evaluation of depositional environment of Parh Limestone, Southern Pab Range, Balochistan, Pakistan. SPE/PAPG Annual Technical Conference, Islamabad; pp. 1-9.

Nichols, G. (2023): Sedimentology and stratigraphy. 3rd edition, John Wiley and Sons Inc; 525p.

Ojo, O.J. and Akande, S.O. (2009): Sedimentology and depositional environments of the Maastrichtian Patti Formation, southeastern Bida Basin, Nigeria. Cretaceous Research; 30(6): 1415-1425.

Özer, S. and Kahrıman, H.H. (2019): Cenomanian canaliculate rudists (Bivalvia) from the GeyikDağı-Hadim area (Central Taurides, S Turkey): Systematic paleontology, stratigraphic importance and depositional environment. Cretaceous Research; 103: 104161.

Peters, K.E., Walters, C.C. and Moldowan, J.M. (2005): The biomarker guide: Biomarkers and isotopes in petroleum exploration and Earth history. 2nd edition, Cambridge University Press; 471p.

Pigott, J.D., Kang, M.H. and Han, H.C. (2013): First order seismic attributes for clastic seismic facies interpretation: Examples from the East China Sea. Journal of Asian Earth Sciences; 66: 34-54.

Poulton, S.W. and Canfield, D.E. (2011): Ferruginous conditions: A dominant feature of the ocean through Earth's history. Elements; 7(2): 107-112.

Ratcliffe, K.T., Morton, A.C., Ritcey, D.H. and Evenchick, C.A. (2007): Whole-rock geochemistry and heavy mineral analysis as petroleum exploration tools in the Bowser and Sustut basins, British Columbia, Canada. Bulletin of Canadian Petroleum Geology; 55(4): 320-336.

Shaltami, O.R. (2022): Petroleum geochemistry of the Benghazi Basin. 1st edition, Lulu Press; 181p.

Shaltami, O.R. (2024): Elemental geochemistry of the Awainat Wanin Formation in three selected areas, Murzuq Basin, SW Libya. Global Scientific Journals (GSJ); 12(2): 992-1016.

Teama, M.A., Kassab, M.A., Cheadle, B.A., Mesbah, M.A., Mohamed, I.F. and El-Din, E.S. (2018): 3D seismic and formation micro-imager (FMI) integrated study to delineate depositional pattern of Abu Madi (Upper Miocene) clastic reservoir rocks in El-Wastani gas field, onshore Nile Delta, Egypt. Egyptian Journal of Petroleum; 27(4): 747-758.

Tucker, M.E. (2001): Sedimentary petrology: An Introduction to the origin of sedimentary rocks. 3rd edition, Blackwell Science; 262p.

Wang, X., Flynn, L.J. and Deng, C. (2023): A review of the Cenozoic biostratigraphy, geochronology, and vertebrate paleontology of the Linxia Basin, China, and its implications for the tectonic and environmental evolution of the northeastern margin of the Tibetan Plateau. Palaeogeography, Palaeoclimatology, Palaeoecology; 628: 111775.

Wedepohl, K.H. (1978): Manganese: abundance in common sediments and sedimentary rocks. In Wedepohl, K.H. (eds), Handbook of Geochemistry: Berlin, Springer; II/3: 1-17.

Zhang, K.J., Li, Q.H., Yan, L.L., Zeng, L., Lu, L., Zhang, Y.X., Hui, J., Jin, X. and Tang, X.C. (2017): Geochemistry of limestones deposited in various platetectonic settings. Earth-Science Reviews; 167: 27-46.

Zhang, M.M., Liu, Z.J., Xu, S.C., Sun, P.C. and Hu, X.F. (2013): Element response to the ancient lake information and its evolution history of argillaceous source rocks in the Lucaogou Formation in Sangonghe area of southern margin of Junggar Basin. Journal of Earth Science; 24(6): 987-996.

Zhou, S. and Huang, H. (2008): Controls on alkylphenol occurrence and distribution in oils from lacustrine rift basins in East China. Science in China Series D: Earth Sciences; 51(7): 976-983.